



Influences of filler dispersity in epoxy resin on the electrical and mechanical performances of embedded capacitance materials

Weikai Zheng¹ · Hong Chen¹ · Xu Zhou¹ · Rui Liu¹ · Gang Jian¹ · Hui Shao¹ · Fengwei Wang¹ 

Received: 8 June 2018 / Accepted: 20 August 2018 / Published online: 22 August 2018
© Springer Science+Business Media, LLC, part of Springer Nature 2018

Abstract

Except for the intrinsic dielectric property of the dielectric filler, its dispersity in polymer matrix also has a big impact on the electrical and mechanical performances of an embedded capacitance material (ECM). Various dielectric fillers are investigated to find the influences of the type and size on the anti-sedimentation and viscosity decreasing properties of the prepared suspensions. The 0.3 μm barium titanate (BaTiO_3) synthesized by hydrothermal method shows the optimal effects in preparing dielectric suspension. And the fabricated ECM show the highest electrical and mechanical performances. Embedded capacitors with different sizes are further processed with low changing ratios under 10%. Reliability tests are also conducted to verify the applicability of the ECM in electronic products. This work shows the importance of the well dispersity of dielectric filler in polymer matrix and provides an efficient method for selecting dielectric fillers suitable for ECM fabrication.

1 Introduction

Conventional discrete components cannot meet the fast-developing requirements of electronic devices, including multifunctionality, size reduction, enhanced signal stability, etc [1–3]. In almost all the electronic devices, passive components take a rather high number proportion, which makes the technical development of advanced passive components an urgent task and a hotspot for worldwide researchers [4–6]. Especially, embedded capacitance materials (ECMs), as the substitution of the most commonly used discrete capacitors, have been already applied in electronic frontiers as aerospace and smart phones. EMCs have a sandwich structure with two layers of copper foil as electrodes and the middle layer as the dielectric material. Instead of solder joints introduced by surface mounted technology (SMT), the ECMs can be connected by copper filled through/blind via holes,

which brings in advantages as lower cost, smaller size, flexible assembly, increased performance and reliability [7–9].

Significant efforts have been devoted to the fabrication of ECMs, especially in developing novel dielectric materials for a higher permittivity and lower dielectric loss. Polyimide (PI) or poly(vinylidene fluoride) (PVDF) are used as polymer matrix, but in most cases only limited effects can be achieved due to the intrinsic low permittivity values. Besides, harsh processing conditions as high temperature and compatibility of different components are difficult to handle [10, 11]. Inorganic fillers with higher polarity such as doped barium titanate or doped strontium titanate are also used to improve the dielectric properties [12–16]. The higher permittivity comes from the inherent anisotropy, which will cause the fillers to aggregate. Thus, it is still a big challenge for researchers to obtain a well dispersed suspension. Conductive nanoparticles can be introduced in the dielectric systems which can form a conductive network in the polymer matrix [17, 18]. When the filling amount reaches the percolation thresholds, the permittivity can have a distinct increase while usually accompanied by a larger dielectric loss [19, 20]. Although chemical modification or other methods have been developed to decrease the contact of conductive nanoparticles, the dedicate filling amount near the percolation threshold is hard to control [21, 22]. 1D/2D carbon materials have also been used to fabricate composite materials with excellent dielectric properties due to their

Electronic supplementary material The online version of this article (<https://doi.org/10.1007/s10854-018-9908-0>) contains supplementary material, which is available to authorized users.

✉ Fengwei Wang
fwwang@just.edu.cn

¹ School of Materials Science and Technology, Jiangsu University of Science and Technology, Zhenjiang 212003, Jiangsu, China

high aspect ratio and lower filling content [23]. Especially for graphene nanosheets, which can improve the dielectric properties below their percolation threshold based on the micro-capacitor model theory [24]. However, the size of these carbon materials is usually too large for application in ECMs, which may bring in risks as decreasing the breakdown voltage. Some new strategies have been proposed for large scale synthesis of nanosized graphene, which may provide a promising solution to the above problems [25].

Most of the former researches are concerned on the development of advanced fillers or polymer matrix with higher dielectric properties. Actually, the well dispersion of dielectric filler in polymer matrix plays a more important role in the fabrication of ECM with excellent electrical and mechanical performances, which is still a big challenge and seldomly involved in reported papers [26, 27]. Commercially available hyperdispersant suitable for dispersing inorganic fillers are preferred instead of commonly applied chemical modification agents. Because special macromolecular block structures of hyperdispersant may bring in well anti-sedimentation as well as effective deflocculation property by physical attraction between the inorganic fillers and the polymer solutions. Without the influences of other chemical additives, we can evaluate the effect in fabrication of ECMs by different kinds of inorganic dielectric fillers following similar fabrication procedures.

Herein, by using the epoxy resin as the basic polymer matrix, barium titanate of different sizes, synthetic methods, doping elements, strontium titanate and doped strontium titanate are compared as dielectric fillers to evaluate the electrical and mechanical performances of ECMs with the addition of hyperdispersant. The stability and viscosity of the prepared suspensions are investigated. And corresponding ECMs are fabricated to evaluate their electrical and mechanical performances. The $0.3\ \mu\text{m}$ BaTiO_3 synthesized

by hydrothermal method is found the most suitable candidate. Processing of embedded capacitors with different sizes and reliability tests of the fabricated ECM are further conducted to confer its applicability in electronic products. The fabrication procedures are shown in Scheme 1.

2 Experimental

2.1 Materials

ED copper foil (1 oz) is purchased from ITEQ (Guangzhou) Corp. Dielectric fillers are supplied by Shanghai Dianyong Industry Co., Ltd. Epoxy resin (E-44) and the matching curing agent are purchased from Chuzhou Huisheng Electronic Materials Co., Ltd. Dry film (H-9030) is purchased from Hitachi Ltd. Hyperdispersant BYK-110 is purchased from BYK Additives & Instruments.

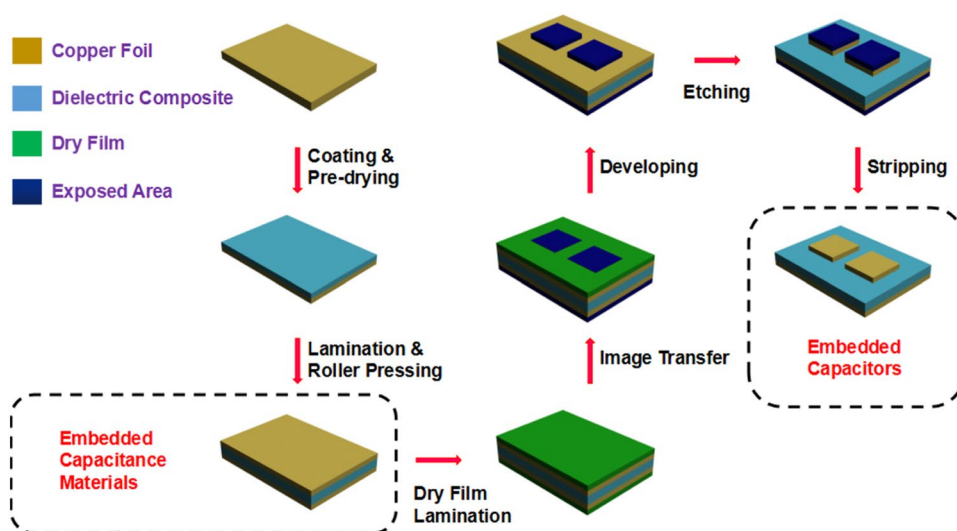
2.2 Preparation of composite suspensions

24 g of dielectric filler is dispersed in a 200 mL 2-butanone solution containing 2 g of BYK-110 followed by ultrasonication for about 30 min to disassociate the agglomeration. Then, 20 ml 2-butanone solution containing 8 g of E-44 and 6 g of the matching curing agent is added and stirred for another 30 min. After the volume reduces to 1/2 by evaporation, composite suspensions containing different dielectric fillers can be obtained.

2.3 Fabrication of embedded capacitance materials

The composite suspension is coated onto the copper foil by a bar coating and dried in an oven at $150\ ^\circ\text{C}$ for 3 min. Then,

Scheme 1 The fabrication procedures of embedded capacitors



two pieces of the above composite films are laminated by a roller press and further cured at 170 °C for 1 h.

2.4 Fabrication of embedded capacitors

The fabricated ECM is pretreated to remove the oxides and contaminations. Then, dry films are laminated onto both sides of the ECM by a roller press. The bottom side is exposed directly for protection of the whole copper foil. The upper side is exposed with designed images according to the laser direct imaging data. Then, developing, etching, stripping and drying are conducted sequentially to obtain embedded capacitors of different sizes (5 × 5 mm, 4 × 4 mm, 3 × 3 mm, 2 × 2 mm, 1 × 1 mm).

2.5 Characterization

The sedimentation ratio (*SR*) is calculated according to the following formula, in which V_1 represents the volume of the upper clear liquid, V_2 represents the volume of the lower turbid liquid.

$$SR = \frac{V_1}{V_1 + V_2} \times 100\%$$

The viscosity of the prepared suspensions is tested by a digital display viscometer (NDJ-9S). The morphologies and the element compositions of ECMs are characterized on a JEOL6010 scanning electron microscope (SEM) equipment with energy-dispersive spectrometry (EDS). The capacitances of the embedded capacitors are measured on a TH2811B LCR meter (Tonghui Electronics). The capacitor number of 100 per size are measured for electrical tests. The peel strength test is conducted on a DZC-5 peel strength tester (Acedo) according to the IPC-TM-650 2.4.9. The temperature/humidity test (85 °C/85% for 1000 h) and temperature cycling test between –40 and 85 °C (100 cycles) is conducted on TH-800 testing box. The reflow soldering test is conducted on a V-TOP1020N reflow oven. Metallography is obtained on ZESS metallurgical microscopy. The high voltage resistance test is conducted on a 5051 Å voltage resistance tester.

3 Results and discussion

SEM images of different dielectric fillers are shown in Fig. 1. BaTiO₃ synthesized by solid reaction process (Fig. 1a–d) show a relative wider size distribution by comparison with hydrothermal synthesized BaTiO₃ (Fig. 1e). SrTiO₃ is also found owning good size distribution (Fig. 1f), while large aggregations can be detected in Ba_xSr_{1-x}TiO₃ (Fig. 1g) as well as in Mg doped Ba_xMg_{1-x}TiO₃ and Sr_xMg_{1-x}TiO₃

fillers (Fig. 1h, i). Mg or Sr elements are doped in fillers, as Mg element can be introduced to increase the dielectric constant and Sr element can be introduced to decrease the dielectric loss and increase the temperature stability of the fillers. The dispersity of dielectric fillers in epoxy resin depends largely on their physical and chemical properties. To get a simple relationship between the dielectric fillers and ECMs, the same hyperdispersant BYK-110 is applied while other fabrication processes remain the same (Figure S1).

The stability of a composite suspension reflects the dispersive status of dielectric filler inside. The sedimentation of dielectric fillers will result in the stratification of composite suspension, affecting the electrical and mechanical properties of the fabricated ECMs. For BaTiO₃ (0.3 μm, 0.4 μm, 0.8 μm) synthesized by solid reaction process, the sedimentation ratio increased from 17.6 to 45.5% with the filler size. The increased sedimentation ratio of 0.1 μm BaTiO₃ may be attributed to the aggregation of the fillers with higher surface free energy. By comparison with the above 0.3 μm BaTiO₃ filler, the 0.3 μm BaTiO₃ filler synthesized by hydrothermal method shows the best anti-sedimentation performance of 2.1%. The better size distribution of the filler can reduce the aggregation of smaller particles and sedimentation of larger particles. Moreover, the rounder shape of the hydrothermal synthesized BaTiO₃ will have a lower surface free energy, which is also beneficial to a better dispersion. The 0.3 μm SrTiO₃ also shows an excellent anti-sedimentation performance of 3.6%, the lower density makes the fillers easier being stabilized in the suspension. However, the doping of 0.3 μm BaTiO₃ by Sr or Mg largely increases the sedimentation ratios, which can be attributed to aggregation of fillers caused by difficulty in controlling the doping homogeneity (Fig. 2).

Generally, composite suspension with good performance shows relative low viscosity due to the well dispersion of dielectric fillers. The 0.3 μm BaTiO₃ (hydrothermal method) and 0.3 μm SrTiO₃ show low viscosity of 30 and 36 mPa s at rotation speed of 60 rpm. Other dielectric fillers show corresponding trends with the sedimentation ratios. However, the 0.8 μm BaTiO₃ show the lowest viscosity of 8 mPa s, which may be caused by the serious sedimentation of fillers of large size. All the suspension systems show thixotropic phenomenon, which are ascribed to mutual interactions between dielectric fillers. The measured components are mainly epoxy resin solutions by using 0.8 μm BaTiO₃ as the filler, which can be verified by the small size of the thixotropic area (Fig. 3).

The prepared suspensions with different dielectric fillers are used to fabricate ECMs (Figure S2). Cross section SEM images of different ECMs show a sandwich structure with copper layers outside and dielectric composite layer inside. All the ECMs show a layer thickness about 10–20 μm. The dielectric fillers can be well dispersed in epoxy resin. And

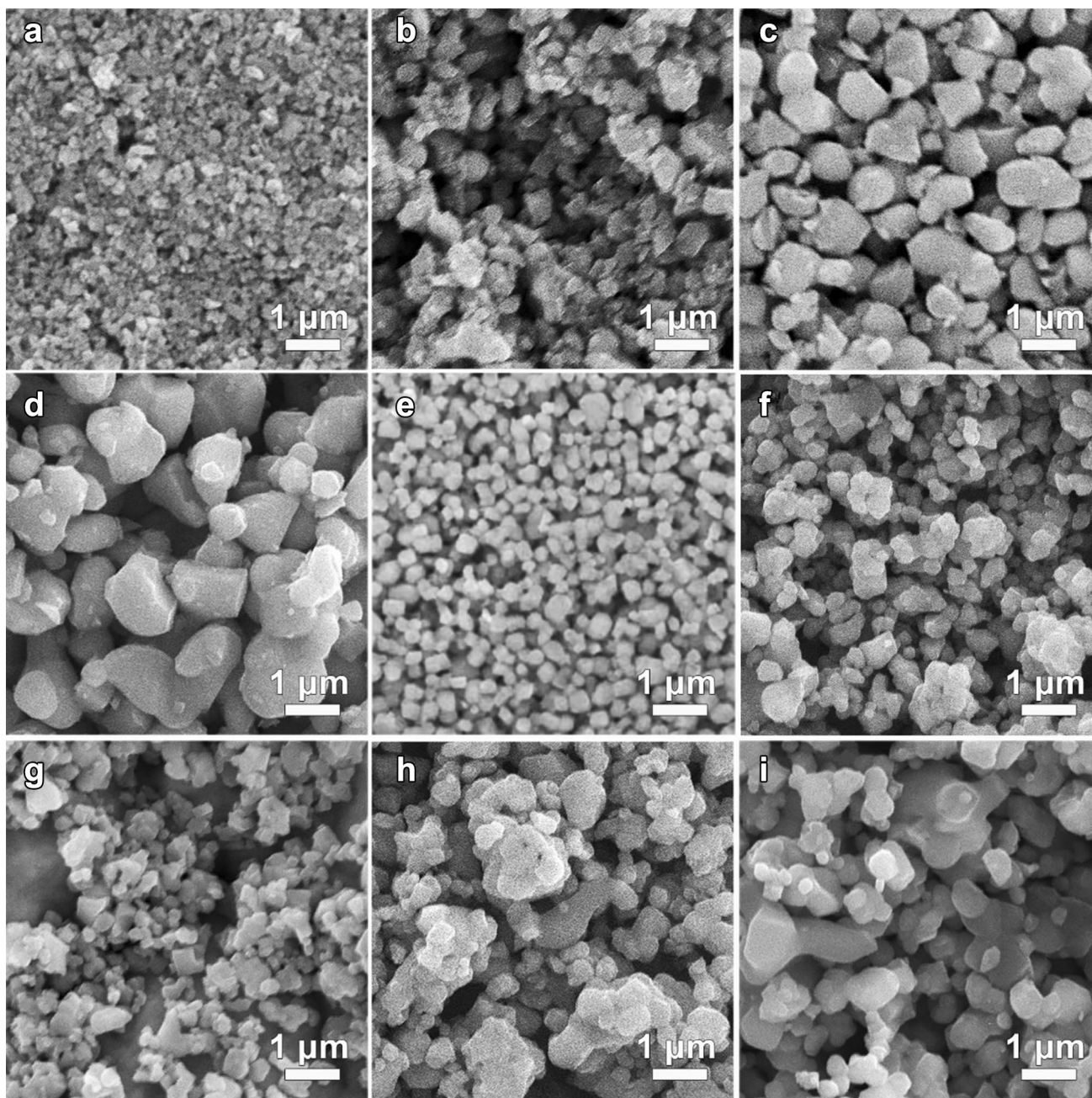


Fig. 1 SEM images of BaTiO_3 of different sizes synthesized by solid reaction process: **a** 0.1 μm ; **b** 0.3 μm ; **c** 0.4 μm ; **d** 0.8 μm ; **e** SEM image of 0.3 μm BaTiO_3 synthesized by hydrothermal method; SEM

image of **f** 0.3 μm SrTiO_3 ; **g** 0.3 μm $\text{Ba}_x\text{Sr}_{1-x}\text{TiO}_3$ SEM; **h** 0.3 μm $\text{Ba}_x\text{Mg}_{1-x}\text{TiO}_3$; **i** 0.3 μm $\text{Sr}_x\text{Mg}_{1-x}\text{TiO}_3$

we can have a clearer view on the size distribution of different dielectric fillers, which is in accordance with the former description (Fig. 4).

The embedded capacitors of 5×5 mm are applied to investigate the dielectric properties of different ECMs.

All ECMs show decreased dielectric constant with frequency (Fig. 5). The obtained dielectric constant depends on the intrinsic dielectric property of the fillers and their dispersive status in epoxy matrix. The 0.3 μm BaTiO_3 (hydrothermal method) ECM shows the highest dielectric

Fig. 2 Sedimentation Ratios of different dielectric fillers: (a) 0.1 μm BaTiO_3 ; (b) 0.3 μm BaTiO_3 ; (c) 0.4 μm BaTiO_3 ; (d) 0.8 μm BaTiO_3 ; (e) 0.3 μm BaTiO_3 (hydrothermal method); (f) 0.3 μm SrTiO_3 ; (g) 0.3 μm $\text{Ba}_x\text{Sr}_{1-x}\text{TiO}_3$ SEM; (h) 0.3 μm $\text{Ba}_x\text{Mg}_{1-x}\text{TiO}_3$; (i) 0.3 μm $\text{Sr}_x\text{Mg}_{1-x}\text{TiO}_3$

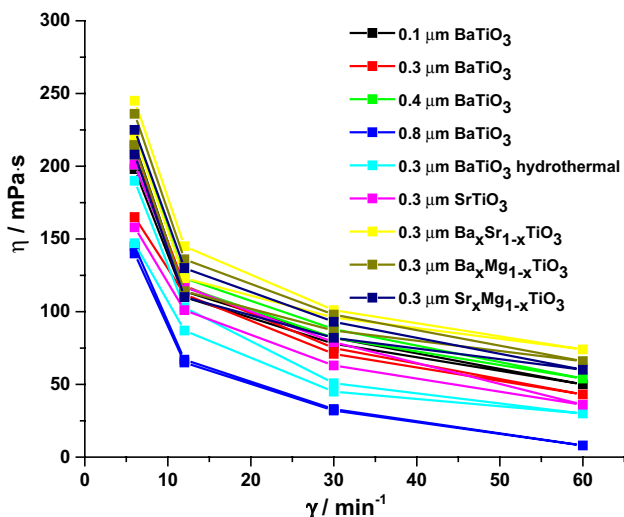
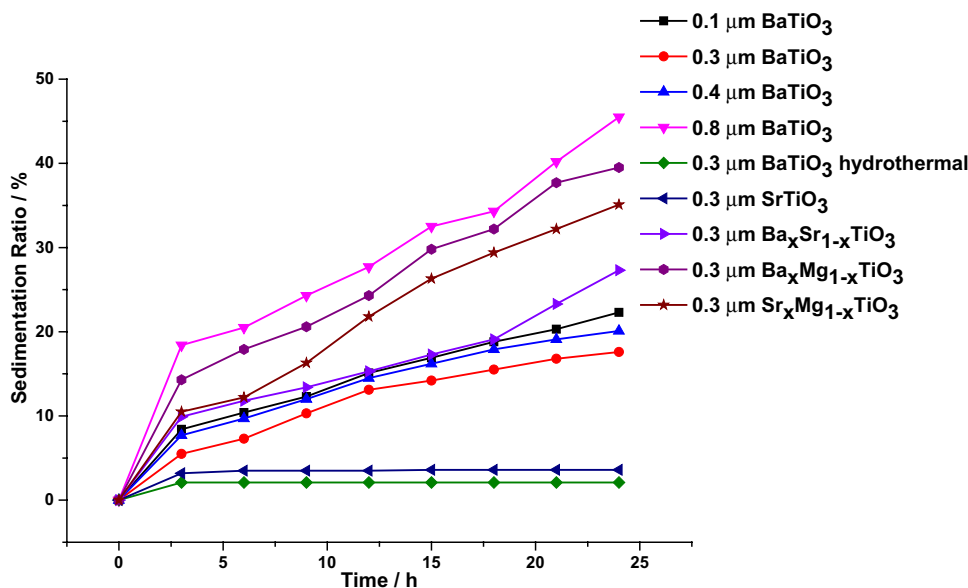


Fig. 3 Dynamic viscosity by using different dielectric fillers: (a) 0.1 μm BaTiO_3 ; (b) 0.3 μm BaTiO_3 ; (c) 0.4 μm BaTiO_3 ; (d) 0.8 μm BaTiO_3 ; (e) 0.3 μm BaTiO_3 (hydrothermal method); (f) 0.3 μm SrTiO_3 ; (g) 0.3 μm $\text{Ba}_x\text{Sr}_{1-x}\text{TiO}_3$ SEM; (h) 0.3 μm $\text{Ba}_x\text{Mg}_{1-x}\text{TiO}_3$; (i) 0.3 μm $\text{Sr}_x\text{Mg}_{1-x}\text{TiO}_3$

constant of 22.7 at 10 KHz. For ECMs using BaTiO_3 synthesized by solid reaction process, the 0.3 μm BaTiO_3 ECM show the best dielectric constant of 19.1 at 10 KHz. While the 0.8 μm BaTiO_3 ECM show the lowest dielectric constant of 15.3 at 10 KHz, which is attributed to its poor

dispersity and anti-sedimentation property. Although the SrTiO_3 has a well dispersive property, the corresponding ECM only show a dielectric constant of 17.3 at 10 KHz due to its intrinsic lower dielectric property. Generally, doping will increase the polarity of BaTiO_3 , which is beneficial to the improvement of the dielectric constant. However, the doping process is usually hard to control for volume production, doping elements can be found in big aggregates, resulting in the decrease of the dispersity, which can be seen in the EDS analysis in Figure S3.

The dielectric loss of all the ECMs are also investigated. The high Sr containing dielectric fillers (0.3 μm SrTiO_3 and $\text{Sr}_x\text{Mg}_{1-x}\text{TiO}_3$) ECMs show high dielectric loss up to 0.6 and 0.754 at low frequency of 100 Hz and relative low values of 0.005 and 0.022 at 10 KHz. The $\text{Ba}_x\text{Sr}_{1-x}\text{TiO}_3$ ECM also show the similar trends with SrTiO_3 and $\text{Sr}_x\text{Mg}_{1-x}\text{TiO}_3$, but the dielectric loss at 100 Hz is not as high the other two ECMs, which may be ascribed to the lower Sr percentage. Other ECMs show smaller dielectric loss changes with frequency. The $\text{Ba}_x\text{Mg}_{1-x}\text{TiO}_3$ show high dielectric loss of 0.063 even at 10 KHz because of the doped conductive Mg element. All BaTiO_3 ECMs show fine dielectric loss below 0.055 in the measured frequencies. The 0.3 μm BaTiO_3 (hydrothermal method) ECM show the best dielectric loss performances with 0.034 at 100 Hz and 0.02 at 10 KHz (Fig. 6).

Besides of the electric properties of ECMs, the corresponding mechanical properties are also measured. The 0.3 μm BaTiO_3 (hydrothermal method) ECM shows the highest peel

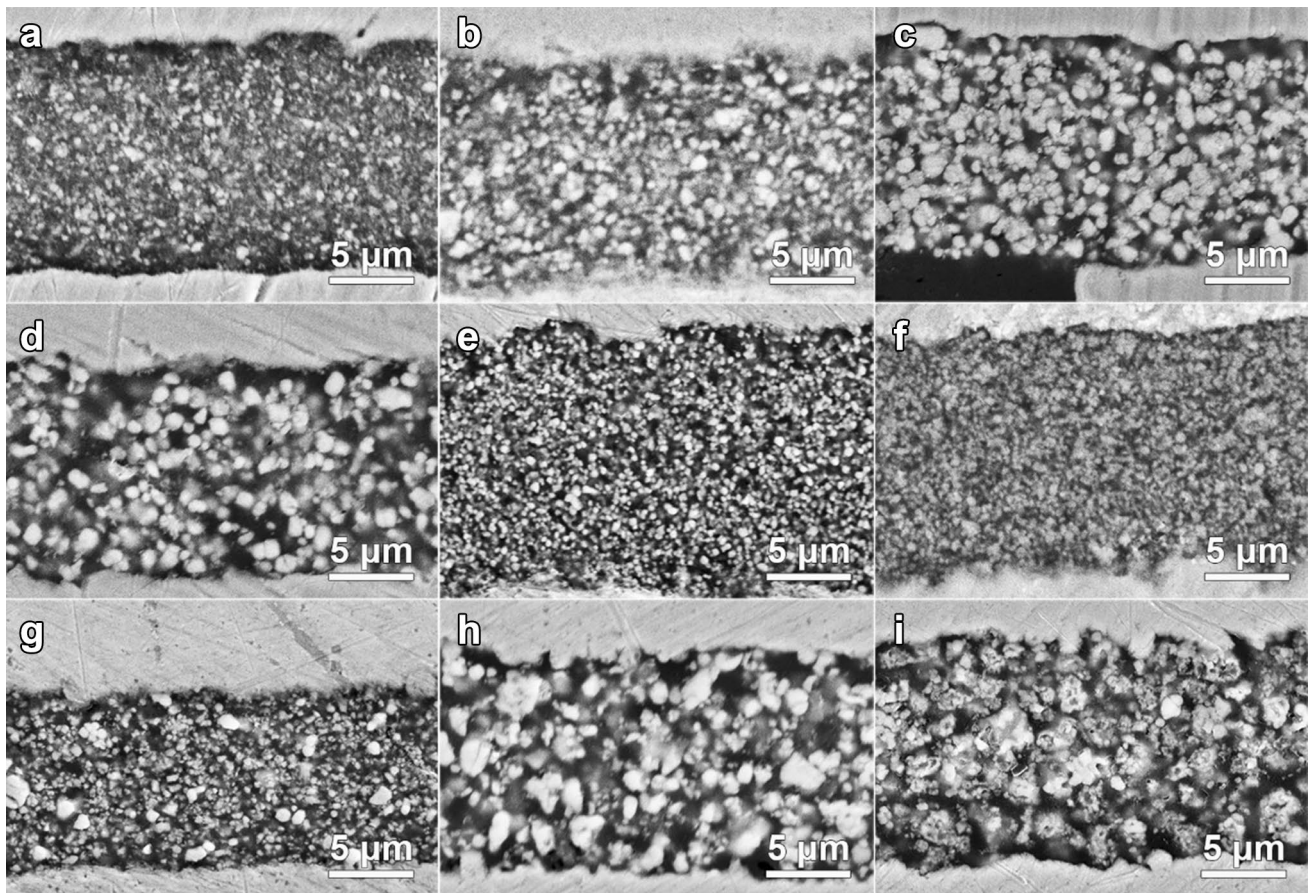
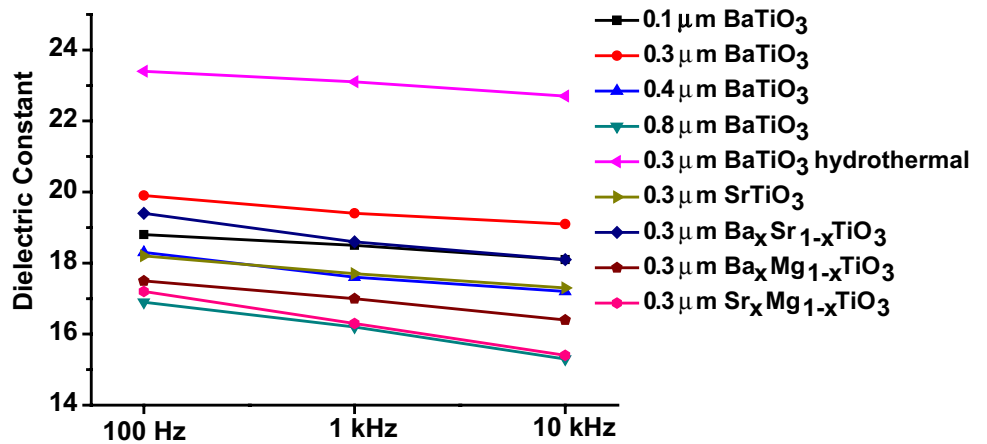


Fig. 4 Cross section SEM images of ECMs fabricated by different dielectric fillers: **a** 0.1 μm BaTiO_3 ; **b** 0.3 μm BaTiO_3 ; **c** 0.4 μm BaTiO_3 ; **d** 0.8 μm BaTiO_3 ; **e** 0.3 μm BaTiO_3 (hydrothermal

method); **f** 0.3 μm SrTiO_3 ; **g** 0.3 μm $\text{Ba}_x\text{Sr}_{1-x}\text{TiO}_3$ SEM; **h** 0.3 μm $\text{Ba}_x\text{Mg}_{1-x}\text{TiO}_3$; **i** 0.3 μm $\text{Sr}_x\text{Mg}_{1-x}\text{TiO}_3$

Fig. 5 Dielectric constant of ECMs fabricated by different dielectric fillers



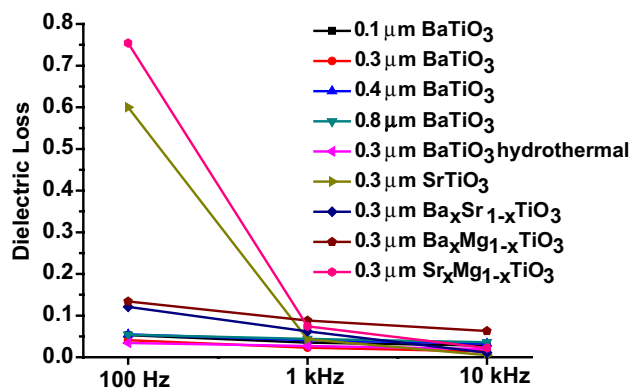


Fig. 6 Dielectric loss of ECMs fabricated by different dielectric fillers

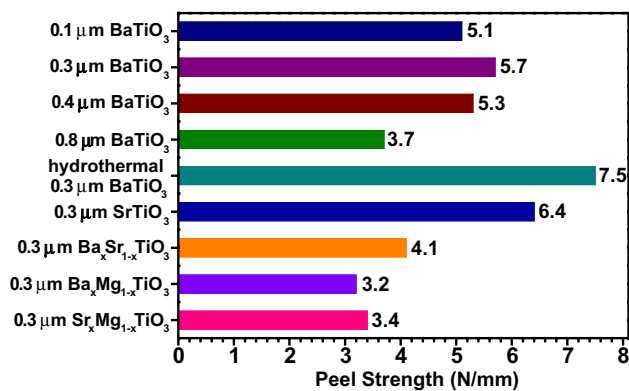


Fig. 7 Peel strength of ECMs fabricated by different dielectric powders

strength of 7.5 N/mm. BaTiO₃ and SrTiO₃ dielectric filler ECMs show peel strength above 5 N/mm, which is necessary for ECM application. While 0.8 μm BaTiO₃ ECM has a low peel strength because of the large filler size caused sedimentation. Other doped dielectric filler ECMs also show poor peel strength owing to the aggregation of fillers (Fig. 7).

From the above analysis, we find the 0.3 μm BaTiO₃ (hydrothermal method) show the best performances in anti-sedimentation and decreasing the viscosity, which is beneficial for volume fabrication of ECM with high dielectric performances. The obtained ECM show dielectric constant of 22.7 and dielectric loss of 0.02 at 10 KHz with low changing ratio with frequency. And the corresponding peel strength shows a high value of 7.5 N/mm. Thus, the fabricated ECM is suitable for fabrication of embedded capacitors.

In this work, five different sizes are fabricated to evaluate the capability of 0.3 μm BaTiO₃ (hydrothermal method) ECM applying in processing of embedded capacitors (Fig. 8). The capacitance density shows a small fluctuation trend around 1.4 nF/cm². The capacitance tolerances measured show an increasing trend with decreasing size due to the

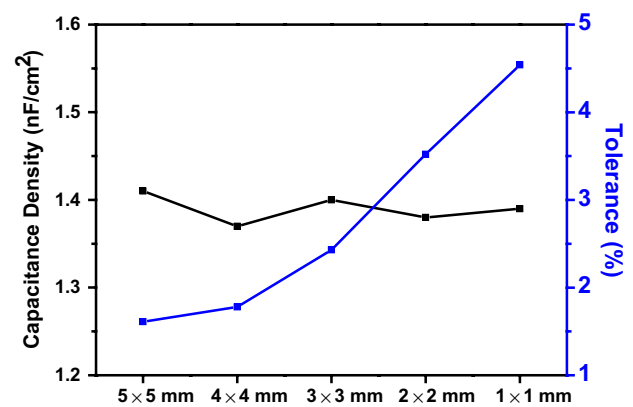


Fig. 8 The capacitance density and corresponding tolerance of embedded capacitor with different sizes fabricated by the 0.3 μm BaTiO₃ synthesized by hydrothermal method

difficulty in control of etching precision. Nevertheless, all the embedded capacitors show low capacitance tolerances below 5%, which is suitable for application in electronic products.

Considering the irreplaceability of embedded capacitors in a completed board, long-term reliability is a major concern of most manufacturers. Capacitance will be changed due to the substrate deformation caused by temperature variation or other processing conditions. In this work, temperature/humidity accelerated aging, temperature cycling, reflow soldering and withstanding voltage test are applied to qualify the test ECM boards fabricated by using 0.3 μm hydrothermal synthesized BaTiO₃ as dielectric fillers.

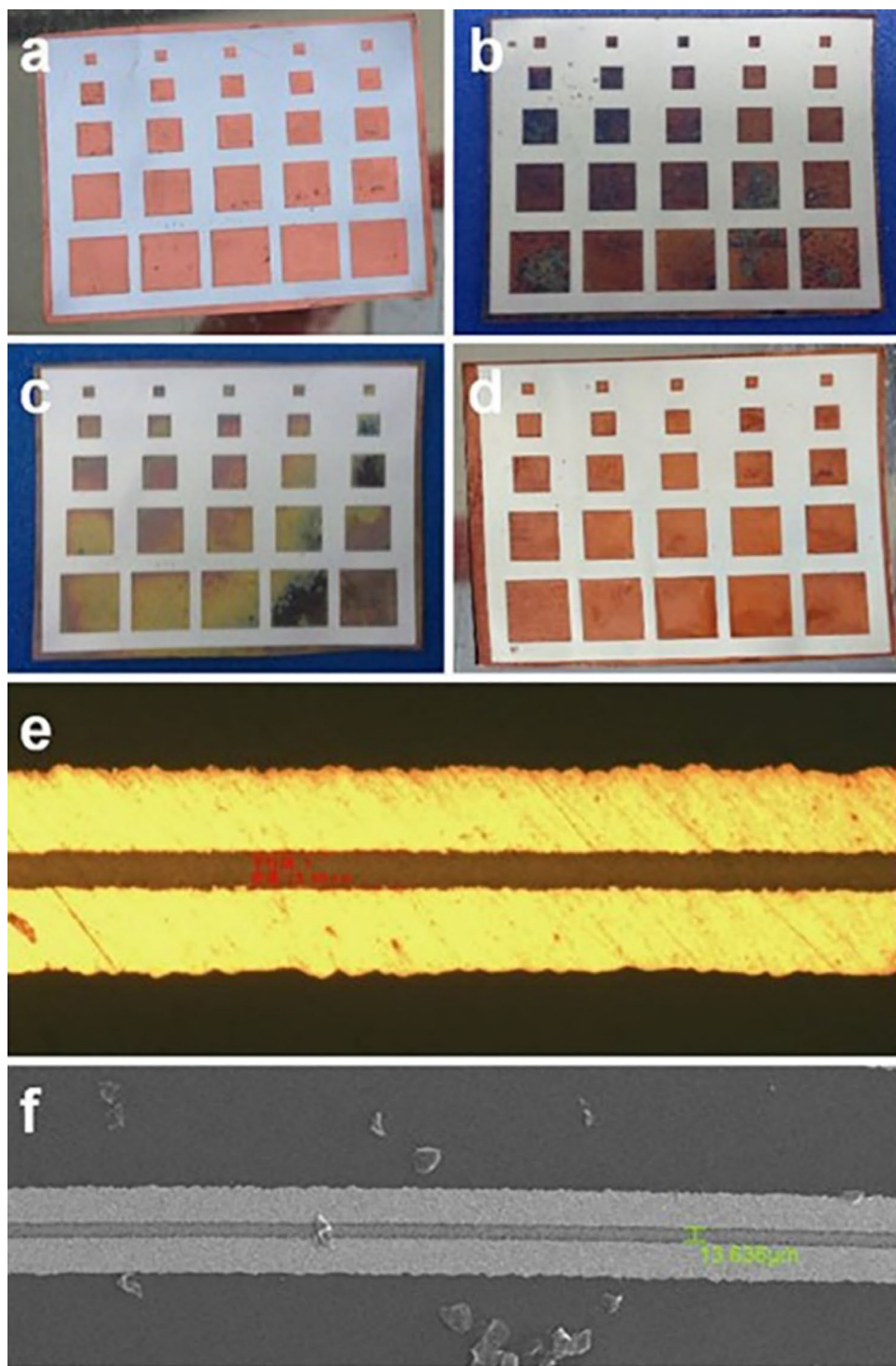
A single piece of embedded capacitor module with different sizes before any reliability test is shown in Fig. 9a. After temperature/humidity accelerated aging, temperature cycling and reflow soldering tests, the module remains robust with only a little surface oxidation of the copper electrodes (Fig. 9b, c), no crack or delamination is detected in the module after the high temperature reflow soldering test with peak temperature above 220 °C (Fig. 9e, f).

The influences of reliability tests show slight decrease in capacitance density for all the embedded capacitor sizes (Fig. 10). No apparent trends are detected with the size. But all the changing ratios can be kept below 10%, which means the fabricated ECM has good reliability (Fig. 11). Moreover, the ECM can pass the high voltage resistance test of 250 V for 60 s, which further confer its applicability in electronic products.

4 Conclusion

In summary, the anti-sedimentation ratio and viscosity of suspensions prepared by dispersing different kinds of dielectric fillers in epoxy resin solution with the presence of

Fig. 9 Photograph of embedded capacitors **a** before treatment; **b** after temperature/humidity aging test; **c** after temperature cycling test; **d** after reflow soldering test. **e** Metallography and **f** SEM images of the cross section of the ECM after reflow soldering test



hyperdispersant are investigated. As a result of the suitable particle size and narrow size distribution, the hydrothermal synthesized $0.3 \mu\text{m BaTiO}_3$ shows the best effects in improving the anti-sedimentation capability and decreasing the viscosity. Electrical and mechanical performances of ECMs fabricated by using the above suspensions are evaluated. Despite of the relative low dielectric property of the

hydrothermal synthesized $0.3 \mu\text{m BaTiO}_3$, the fabricated ECM still show the best performances and can pass the processability and reliability tests, which verifies the applicability in electronic products. This work shows the importance of the well dispersivity of dielectric filler in polymer matrix besides of the intrinsic dielectric properties and provides an

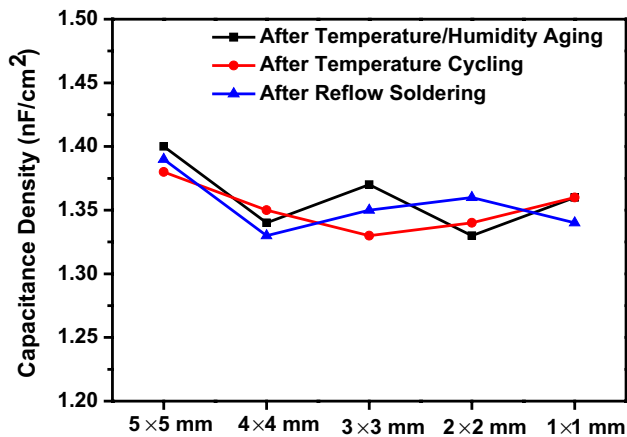


Fig. 10 The change of capacitance density of embedded capacitors after temperature/humidity aging, temperature cycling and reflow soldering tests

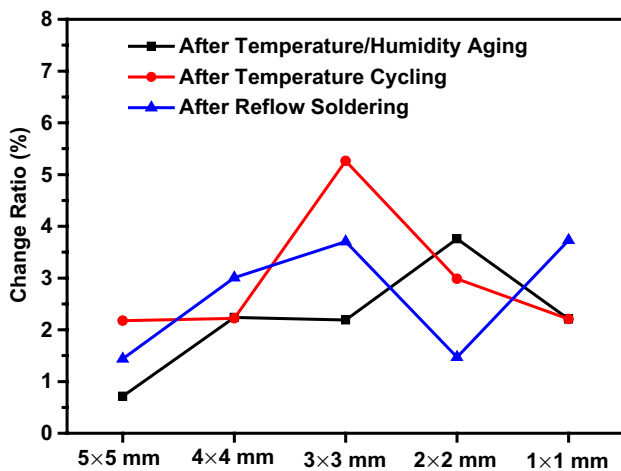


Fig. 11 The change ratio of capacitance density of embedded capacitors after temperature/humidity aging, temperature cycling and reflow soldering tests

efficient method for selecting dielectric fillers suitable for ECM fabrication.

5 Supporting Information

Additional photograph of the coated copper foil, EDS analysis of doped dielectric filler. This material is available free of charge via the Internet at <http://www.springer.com>.

Acknowledgements This work is supported by the Natural Science Foundation of Jiangsu Province (Grant No. BK20170585) and Priority Academic Program Development of Jiangsu Higher Education Institutions (PAPD).

References

1. Y.J. Xiao, W.Y. Wang, T. Lin, X.J. Chen, Y.T. Zhang, J.H. Yang, Y. Wang, Z.W. Zhou, *J. Phys. Chem. C* **120**, 6344 (2016)
2. Reduce PCB impedance, noise, and EMI and simplify PCB layout (2018), <http://www.3Mcapacitance.com>. Accessed 13 May 2018
3. L. Wang, Z.M. Dang, *Appl. Phys. Lett.* **87**, 042903 (2005)
4. B.P. Mahler, B. Lawrence, in *JEDEC G-11 Conference* (2009)
5. A. Dziedzic, *Microelectron. Reliab.* **42**, 709 (2002)
6. F.W. Wang, C.Q. Cui, J. Wang, *J. Mater. Sci.* **26**, 9766 (2015)
7. F.W. Wang, C.Q. Cui, S.T. Wang, J. Wang, *J. Adhes. Sci. Technol.* **30**, 1364 (2016)
8. J.X. Lu, K.S. Moon, J.W. Xu, C.P. Wong, *J. Mater. Chem.* **16**, 1543 (2006)
9. M. Arjmand, S. Sadeghi, M. Khajepour, U. Sundararaj, *J. Phys. Chem.* **121**, 169 (2017)
10. Z.M. Dang, J.K. Yuan, J.W. Zha, T. Zhou, S.T. Li, G.H. Hu, *Prog. Mater. Sci.* **57**, 660 (2012)
11. Z.M. Dang, H.Y. Wang, Y.H. Zhang, J.Q. Qi, *Macromol. Rapid Commun.* **26**, 1185 (2005)
12. T. Hu, J. Juuti, H. Jantunen et al., *J. Eur. Ceram. Soc.* **27**, 3997 (2007)
13. W.H. Yang, S.H. Yu, R. Sun et al., *Acta Mater.* **59**, 5593 (2011)
14. W.H. Yang, S.H. Yu, R. Sun et al., *Ceram. Int.* **38**, 3553 (2012)
15. Z.F. Zhang, X.F. Bai, J.W. Zha, W.K. Li, Z.M. Dang, *Compos. Sci. Technol.* **115**, 87 (2015)
16. S.D. Cho, S.Y. Lee, J.G. Hyun, K.W. Paik, *J. Mater. Sci.* **16**, 77 (2005)
17. Z.M. Dang, Y.H. Lin, C.W. Nan, *Adv. Mater.* **15**, 1625 (2003)
18. Q. Li, L. Chen, M.R. Gadinski, S. Zhang, G. Zhang, H. Li, A. Haque, L.Q. Chen, T. Jackson, Q. Wang, *Nature* **523**, 576 (2015)
19. Z.M. Dang, L. Wang, Y. Yin, Q. Zhang, Q.Q. Lei, *Adv. Mater.* **19**, 852 (2007)
20. B. Wang, L. Liu, L. Huang, L. Chi, G. Liang, L. Yuan, A. Gu, *Carbon* **85**, 28 (2015)
21. P.H. Hu, Y. Shen, Y.H. Guan, X.H. Zhang, Y.H. Lin, Q.M. Zhang, C.W. Nan, *Adv. Funct. Mater.* **24**, 3172 (2014)
22. A. Ameli, S. Wang, Y. Kazemi, C.B. Park, P.A. Patschke, *Nano Energy* **15**, 54 (2015)
23. S. Stankovich, D.A. Dikin, G.H.B. Domment, K.M. Kohlhaas, E.J. Zimmey, E.A. Stach, R.D. Pinner, S.T. Nguyen, R.S. Ruoff, *Nature* **442**, 282 (2006)
24. L. Jiao, L. Zhang, X. Wang, G. Diankov, H. Dai, *Nature* **458**, 877 (2009)
25. P. Pachfule, D. Shinde, M. Majumder, Q. Xu, *Nat. Chem.* **8**, 718 (2016)
26. R. Ruppin, *Solid State Commun.* **116**, 411 (2000)
27. Y.J. Li, M. Xu, J.Q. Feng, *Appl. Phys. Lett.* **89**, 072902 (2006)